Journal of Materials Chemistry C

Investigating the Active Layer Thickness Dependence of Non-Fullerene Organic Solar Cells Based on PM7 Derivatives

Journal:	*Journal of Materials Chemistry C*
Manuscript ID	TC-ART-06-2020-003096.R2
Article Type:	Paper
Date Submitted by the Author:	05-Oct-2020
Complete List of Authors:	Jones, Austin; Georgia Institute of Technology, Chemistry and Biochemistry Ho, Carr Hoi Yi; North Carolina State University Riley, Parand; North Carolina State University Angunawela, Indunil; North Carolina State University Ade, Harald; North Carolina State University, Physics So, Franky; North Carolina State University, MSE Reynolds, John; Georgia Institute of Technology, Chemistryand Biochemistry, Materials Science and Engineering

Investigating the Active Layer Thickness Dependence of Non-Fullerene Organic Solar Cells Based on PM7 Derivatives

Austin L. Jones[†], Carr Hoi Yi Ho[‡], Parand R. Riley[‡], Indunil Angunawela[⊥], Harald Ade[⊥], Franky So[‡] and John R. Reynolds[†]

[†]School of Chemistry and Biochemistry, School of Materials Science and Engineering, Center for Organic Photonics and Electronics, Georgia Tech Polymer Network, Georgia Institute of Technology, Atlanta, Georgia 30332, United States.
[‡]Department of Materials Science, Engineering, Organic, and Carbon Electronics Laboratories (ORaCEL), North Carolina State University, Raleigh, North Carolina 27695, United States.
[⊥]Department of Physics, Organic and Carbon Electronics Laboratories (ORaCEL), North Carolina State University, Raleigh, North Carolina 27695, United States.

Abstract. Power conversion efficiencies (PCEs) in organic solar cells (OSCs) have rapidly improved in the last 5 years owing largely to the development of novel small molecule acceptors and polymer donors with several systems performance exceeding 17%. A key factor for these materials implementation into industrial relevant devices is their active layer thickness tolerance as solar cell performances are typically reported with thicknesses on the order of 100-150 nm, but thicker films (ca. 300 nm) are needed for printing and roll-to-roll processing. In this report, two PM7 isomeric derivatives were synthesized featuring a chlorinated benzodithiophene and ester functionalized terthiophene moieties for the incorporation into non-fullerene OSCs. The fundamental difference between the two isomeric polymers is the location of the ester side chains where the PM7 D1 esters are located on the outer thiophene units, whereas the esters on PM7 D2 are located on the central thiophene unit. This simple modification produced polymers with similar absorption profiles, electrochemical onsets, mobilities when blended with ITIC-4F, and grazing-incidence wide-angle x-ray scattering patterns. Thin-film (100 nm) OSCs were fabricated resulting

in average PCEs of 11.6% for PM7, 12.1% for PM7 D1, and 9.9% for PM7 D2 when blended with ITIC-4F. In contrast, large differences are observed in PCE when the active layer thickness is increased to 180 nm resulting in a decrease in average PCE for PM7 D2 (5.3%), whereas PM7 D1 was able to retain a 11.9% average PCE. The difference in active layer thickness tolerance between PM7 D1 and PM7 D2 is rationalized by extracting the energetic disorder (σ) for hole transport using temperature dependent space-charge limited current studies. In the end, this study conveys how small changes to polymer structure, such as side chain placement, may have a small effect on thin-film polymer properties and device performance, but significant differences are realized when charges are transported over longer distances (thicker films, > 150 nm).

1. Introduction

Organic solar cells (OSCs) comprised of solution processable, synthetically modified donor and acceptor semiconductors mixed in a bulk heterojunction (BHJ) have represented a promising, sustainable, and green energy alternative.[1-4] Blending a p-type conjugated polymer donor with a n-type, small-molecule, non-fullerene acceptor (NFA) in a BHJ have represented the most promising active layer materials to date, with power conversion efficiencies (PCE) reaching 17% in single junction OSCs.[5-9] The recent improvement in PCE of OSCs has largely been influenced by the advancement in the synthetic modification of fused-ring electron acceptors (FREAs) which possess several advantages including strong visible-near-infrared (NIR) absorption, electrochemical and structural flexibility, and facile synthesis and purification.[10-11] Since the first FREA, ITIC, was synthesized in 2015 by the Zhan group,[12] many alterations have been made to the electron rich core, electron deficient end-groups, and/or side chain to modify the NFAs compatibility with polymeric donors.[13-17] In 2017, a fluorinated derivative (ITIC-4F) of ITIC was synthesized which, at the time, produced state-of-the-art OSC devices due in part to the

further red-shifted absorption, deeper highest occupied molecular orbital (HOMO) level, and improved BHJ morphology.[18] The ITIC-4F NFA was one of the highest performing acceptor-donor-acceptor (ADA) electron-rich core FREA, but recently a new structure paradigm, which produced higher PCEs, was designed where an electron-deficient core FREA was synthesized to give an overall acceptor-donor-acceptor-donor-acceptor (ADADA) motif.[19-25] Incorporation of an electron-deficient unit in the FREA core allowed for increased conjugation length without significantly raising the HOMO level of the NFA, therefore, absorption further in the NIR (approaching 1000 nm) was possible without compromising the donor-acceptor ionization energy (IE) alignment.

To maximize solar irradiance consumption, wide-bandgap (WBG) polymer donors are paired with narrow-bandgap NFAs to produce active layer blends with complementary absorption.[26-35] To date, the most successful family of WBG polymer donors (PBDB-T), generally comprised of a benzodithiophene (BDT) donor unit and a benzodithiophene-4,8-dione (BDD) or thiophene ester acceptor unit, were first implemented in a NFA OSC in 2016 by the Hou group when blended with ITIC.[36-38] Since this report, there has been a plethora of PBDB-T derivatives designed with one of the most widely used being the fluorinated version (PM6) where two fluorine atoms were introduced on the conjugated side chain of BDT (Scheme 1).[39-48] Fluorination of the polymer donor enhances the solar cell performance by lowering the HOMO level, thus increasing the open-circuit voltage (V_{OC}), and increasing the carrier mobilities due to stronger intermolecular interactions which can enhance the active layer packing.[42, 49] Recently, chlorine has been found to be a practical replacement for fluorine in both the polymeric donor and NFA components of the active layer blend.[50-60] In comparison with their fluorinated counterparts, chlorinated polymer donors have lower energy levels, decreased energy loss, blue-shifted optical absorption, enhanced

molecular packing, and most importantly, easier synthesis. This was most clearly demonstrated in 2018 when a chlorinated version of PBDB-T (PM7) was synthesized which used three fewer synthetic steps compared to its fluorinated equivalent.[54] This notion of designing economical π-conjugated materials for OSCs has become vital due to PCEs reaching industrial relevance.[61-62] Poly(3-hexylthiophene) (P3HT) is still considered the most cost-effective and industrially relevant polymer donor, but suffers from low PCE mainly due to the low IE which limits V_{OC} and its compatibility with NFAs.[63-65] To resolve this problem, ester functionalized polythiophene derivatives have been synthesized and successfully paired with NFAs to produce high performing OSCs that are still relatively cost-effective, as compared to most top-performing polymer donors.[66-67] Additionally, the thiophene ester moiety has been incorporated into several donor-acceptor (DA) polymers as a relatively simple acceptor unit alternative (Scheme 1).[28, 32-33, 68]

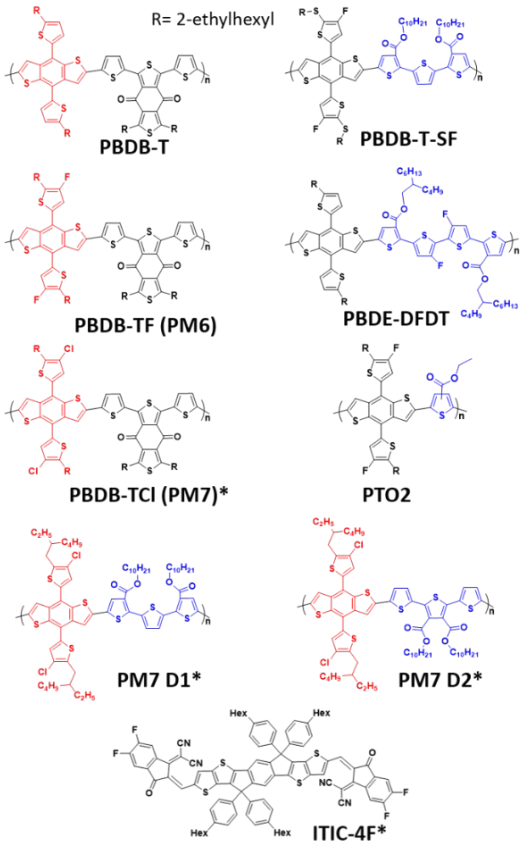

Scheme 1. High performing polymer donors incorporating BDT and thiophene esters from the literature, PM7 D1, PM7 D2 and ITIC-4F. *Materials used in this study.

An equally important challenge in the field of OSCs is designing materials that have a high active layer thickness tolerance as this will be necessary for large-scale device fabrication.[69-72] In general, NFA OSCs have optimal active layer thicknesses around 100 nm and typically experience dramatic performance losses when casted thicker due largely to a loss in fill factor (FF). On the other hand, fullerene-based OSCs have shown less dependence on the active layer thickness, which is attributed to fullerenes large electron mobility and aptitude to form relatively large, semi-crystalline domains.[73-76] Therefore, there has recently been a thrust to design NFA OSC active layers that retards the performance drop when casted as a thicker film through the synthesis of new polymer donors,[77] synthesis of new NFAs,[45, 78-80] and the use of ternary blends.[81-83] Although there have been a few successful reports regarding thick active layer NFA OSCs through new polymer design, there is still a need for the field to check new materials active layer thickness tolerance as many only report one thickness, which may be misleading when considering a materials utility in large scale device fabrication.

In this contribution, two isomeric polymers were synthesized with the vision of creating relatively scalable, high-performing PM7 derivatives which replaces BDD with a terthiophene unit functionalized with ester side chains (Scheme 1). The two derivative polymers differ only in the placement of the ester functionality on the terthiophene moiety where PM7 D1 is functionalized on the outer thiophene units, and PM7 D2 are located on the central thiophene unit. By using parallel polymerization techniques, the three polymers (PM7, PM7 D1 and D2) were isolated with high chemical purity, similar molecular weights and dispersities, which allow for an impartial comparison of material properties, and ultimately device performance. Introducing the oligothiophene ester units decreased polymer aggregation which is reflected in the blue-shifted, structureless absorption profiles creating better complementary absorption when paired with ITIC-

4F (Fig. 1a), compared to PM7. Solar cell fabrication revealed PM7 and PM7 D1 perform similarly (PCE = 12%) and PM7 D2 performs slightly worse (PCE = 10%) when casted as 100 nm-thick active layers. On the other hand, when the active layers were increased to a thickness of 180 nm, the performance of D2 dramatically declined whereas the PCE of D1 was retained. This thickness dependence originates from the polymers stacking ability in the BHJ which, in this case, is determined by the side chain placement along the backbone and can be quantified by characterizing the hole energetic disorder. This work exposes the importance of testing a polymers active layer thickness tolerance as small modifications to a polymers structure, such as side chain placement, can radically change its ability to stack/pack in the BHJ which is reflected in thick active layer OSCs.

2. Results and Discussion

The three polymers featured here were polymerized using traditional Stille cross-coupling conditions in pre-dried, degassed chlorobenzene using tris(dibenzylideneacetone)dipalladium(0) ($Pd_2(dba)_3$) as the palladium source and tri(*o*-tolyl)phosphine (P(*o*-tol)$_3$) as the corresponding ligand. Polymers were isolated in excellent yields (> 90%) after reacting for 24 hours at 140 °C and purified using Soxhlet techniques. High-temperature gel permeation chromatography (GPC) performed in 1,2,4-trichlorobenzene reported number average molecular weights (M_n) between 45 and 50 kg/mol and dispersities ($Đ_M$) below 2.5 with monomodal chromatograms (Table 1). Elemental analysis proved the purity of the polymers as each were within the detection limit (0.3%) of their calculated C, H, and S ratios (Table 1). The similar molecular weight, dispersity, and chemical purity of the three polymers will minimize differences in solubility, molecular packing, and blend morphology to provide a reasonable comparison. The full synthetic procedure, schemes, NMR spectra, and GPC traces are located in the Supporting Information (Figs. S1-S20).

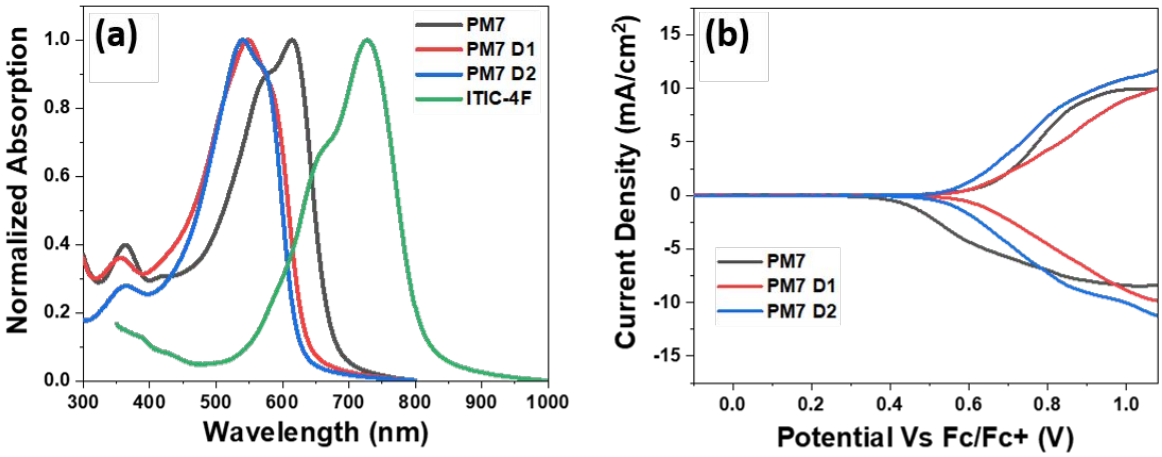

Figure 1. (a) Film UV-vis absorption casted from chlorobenzene. (b) Differential pulsed voltammetry oxidation curves.

Table 1. Percent Yield, GPC and Elemental Analysis

			Elemental Analysis Actual/Theoretical		
Polymer	**Yield (mg)**	**M_n(kg/mol)/$Đ_M$**	**C%**	**H%**	**S%**
PM7	240/93%	48.8/2.45	65.21/65.20	6.24/6.12	20.62/20.47
PM7 D1	235/91%	49.6/2.25	64.67/64.78	6.65/6.72	17.60/17.80
PM7 D2	245/92%	45.8/2.07	64.87/64.78	6.58/6.72	17.74/17.80

The solution (Fig. S21) and thin-film (Fig. 1a) UV-vis absorption spectra show that the reference PM7 polymer is significantly red-shifted as compared to the two terthiophene ester derivatives. As previously shown, polymers in the PBDB-T family show strong solution aggregation due to the planar, 2D BDT and BDD conjugated units which facilitate polymer stacking.[29, 59] Therefore, the PM7 UV-vis in chlorobenzene shows a structured profile with a low energy band at λ_{max}= 608 nm, previously assigned as an aggregation peak, and a high energy band at λ_{max}= 572 that is attributed to the π-π* transition (Fig. S21).[29] In contrast to PM7, the two derivatives (D1 and D2) have identical featureless absorption bands in chlorobenzene with a λ_{max}= 525 nm assigned as the π-π* transition. The structureless absorption bands are likely due to many non-planar conformers with minimal difference in energy brought on by the terthiophene units which possess more degrees of freedom as compared to the BDD unit. This phenomenon has been

previously reported in oligothiophene/polythiophene structures and in the incorporation of oligothiophene units into DA polymers.[28, 84] We note here that PM7 D1 and D2 have identical solution absorption profiles in chlorobenzene, which is desirable when comparing chlorobenzene active layer casted devices. The thin-film absorption spectra for D1 and D2 are red-shifted and reveal a new distinct low energy shoulder that is characteristic of aggregation and planarization of the polymer backbone due to the loss of degrees of freedom present in solution (Fig. 1b). Optical differences are more obvious in the thin-film absorption as absorption onset and λ_{max} of PM7 D1 are slightly lower in energy (E_{gap}^{opt} = 1.93 eV, λ_{max}= 548 nm) as compared to D2 (E_{gap}^{opt} = 1.96 eV, λ_{max}= 540 nm). As noted before, due to the strong aggregation in solution, the thin-film absorption of PM7 is nearly identical to its solution profile with a slight 15 nm red-shift of the onset due to further planarization in the solid state. Finally, the blue-shifted absorption of D1 and D2 compared to PM7 overlap less with ITIC-4F suggesting better complementary absorption when considering the polymers thin-film λ_{max}.

Thin-film redox properties of the three PM7 polymers were characterized using cyclic voltammetry (CV, Fig. S22) and differential pulsed voltammetry (DPV, Figs. 1b and S23). Qualitatively, the cyclic voltammograms look similar for all three polymers with quasi-reversible cathodic and anodic waves. More insight was provided by carefully performing DPV to estimate the IE and electron affinity (EA) values from the onset potentials of each polymer. The onset values were estimated using the first DPV scan, and a fresh film was used for each oxidation and reduction sweep to eliminate changes in the film morphology and swelling effects, as previously published.[85] Interestingly, the onset of oxidation for PM7 and PM7 D1 are nearly identical (E_{onset}^{ox} = 0.62 V) whereas the onset of oxidation for PM7 D2 is slightly lower at E_{onset}^{ox} = 0.57 V, which will most likely translate to a lower V_{OC} when blended with ITIC-4F in a OSC.[86] The difference in oxidation

potential between D1 and D2 suggests that the terthiophene ester motif in D2 behaves as a weaker acceptor unit as compared to D1, this is not obvious by the onset of reduction for D2 (E_{onset}^{red} = -1.8 V) when compared to D1 (E_{onset}^{red} = -1.78 V), according to DPV (Fig. S23). This may suggest that the D1 terthiophene moiety is more "twisted" as compared to D2, resulting in a higher oxidation potential. Taken together, the electrochemical gap for PM7 is smaller E_{gap}^{echem} = 2.33 eV as compared to the two derivatives, D1 and D2, which corroborates well with the smaller optical gap estimated from the onset of absorption (Table S1). With the polymers electrochemically characterized, the IE and EA energy levels were estimated, and an energy level diagram with ITIC-4F was constructed (Fig. S24). A crucial variable to OSCs is the IE energy offset between the donor and acceptor as small offsets may dramatically impact the device performance. The polymers studied here all have a larger than 0.2 eV offset with ITIC-4F which has previously been shown to be sufficient, although not necessary, for optimally performing OSCs.[85]

Inverted BHJ OSCs with a device architecture of indium tin oxide (ITO)/zinc oxide/polymer:ITIC-4F/molybdenum trioxide/silver were fabricated using the three polymers. All active layer solutions consisted of a 1:1 polymer:ITIC-4F weight ratio in CB with a 1% 1,8-diiodooctane (DIO) additive, which is similar to the optimal published conditions for PM7.[54] The current density–voltage (*J-V*) plots and the summary of device characteristics are presented in Figure 2 and Table 2 for both thin (100 nm) and thick (180 nm) active layer devices. First, solar cells with a 100 nm thick active layer were fabricated using all polymers, as this thickness was found to be optimum for PBDB-T:ITIC-4F blend cells.[18, 28, 54, 87-88] Interestingly, PM7 D1 and PM7 performed similarly with average PCEs around 12% with the prime difference in device characteristics being the current density (J_{SC}), which is slightly higher for PM7 D1 (Table 2). In

contrast, the average PCE of PM7 D2 was 2% lower than the other two polymers due to lower FF, J_{SC} and V_{OC}, with the latter predicted from the electrochemical results as PM7 D2 had the lowest oxidation potential onset. Significant differences are observed when the two PM7 derivatives were

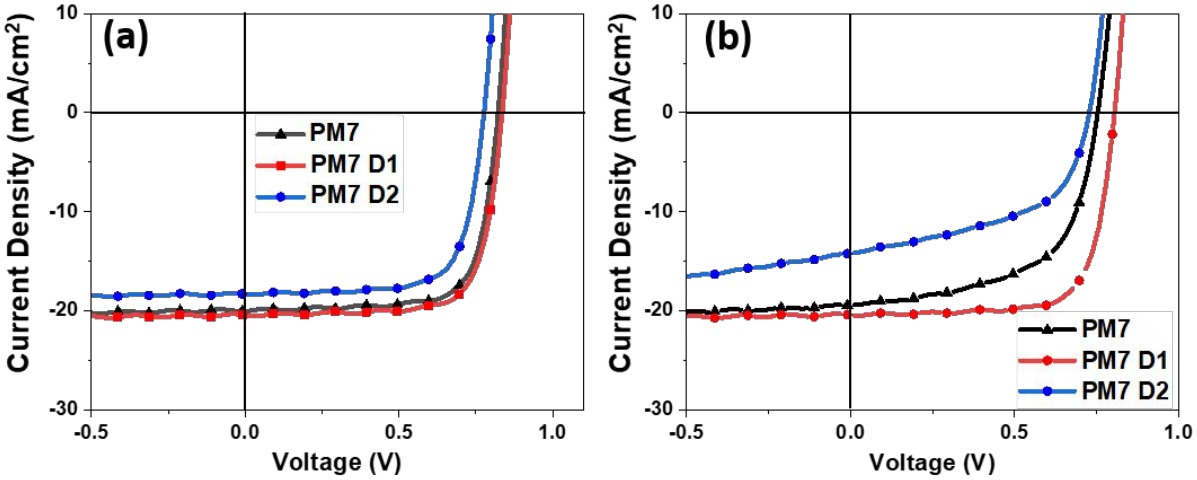

Figure 2. Current density–voltage characteristics of OPV devices with a (a) 100 nm thick and (b) 180 nm thick active layer.

Table 2. Solar Cell Device Characteristics

Polymer (blend thickness, nm)	J_{SC} (mA/cm^2)	V_{OC} (V)	FF (%)	PCE (best) (%)
PM7 (100)	18.9 ± 1.0	0.83 ± 0.01	74 ± 0.5	11.6 ± 0.5 (12.22)
PM7 D1 (100)	19.7 ± 0.7	0.84 ± 0.01	73 ± 2.0	12.1 ± 0.4 (12.78)
PM7 D2 (100)	18.0 ± 0.4	0.78 ± 0.01	71 ± 1.0	9.9 ± 0.2 (10.35)
PM7 (180)[a]	18.4 ± 0.8	0.76 ± 0.01	59 ± 1.0	8.4 ± 0.3 (8.77)
PM7 D1 (180)[a]	19.7 ± 0.4	0.81 ± 0.01	74 ± 1.0	11.9 ± 0.2 (12.20)
PM7 D2 (180)[a]	13.9 ± 0.2	0.74 ± 0.01	52 ± 1.0	5.3 ± 0.1 (5.43)
PM7 (100)	18.7 ± 0.4	0.86 ± 0.01	73 ± 0.3	11.7 ± 0.1 (11.86)
PM7 D1 (100)	19.2 ± 0.9	0.85 ± 0.01	72 ± 2.0	11.7 ± 0.2 (11.83)
PM7 D2 (100)	17.7 ± 0.5	0.82 ± 0.01	70 ± 1.5	10.2 ± 0.2 (10.38)
PM7 (180)	18.9 ± 0.3	0.79 ± 0.01	53 ± 1.5	8.2 ± 0.3 (8.50)
PM7 D1 (180)	20.2 ± 0.6	0.84 ± 0.01	63 ± 1.5	10.6 ± 0.4 (10.94)
PM7 D2 (180)	17.3 ± 0.6	0.77 ± 0.01	48 ± 1.0	6.4 ± 0.3 (6.72)
PM7 (320)[a]	19.7 ± 0.3	0.79 ± 0.01	49 ± 1.8	7.7 ± 0.3 (7.95)
PM7 D1 (320)[a]	20.1 ± 0.3	0.83 ± 0.01	54 ± 0.8	8.8 ± 0.2 (9.03)
PM7 D2 (320)[a]	9.98 ± 0.4	0.79 ± 0.01	47 ± 0.3	3.7 ± 0.2 (3.90)

[a]Thermally annealed at 100 °C for 10 minutes. Results for solar cells fabricated at Georgia Tech are above the horizontal dotted line, while those fabricated at North Carolina State University are below the line, demonstrating close correlation in two device construction laboratories. Devices were averaged over 8 devices and the thicknesses are within ± 10 nm.

casted as thicker films (180 nm) and tested for their OSC performance as PM7 D1 was able to retain its average 12% PCE, whereas PM7 D2 showed a dramatic decrease to 5.3%. Here we note that in order to optimize the thick-film active layers, a 10-minute thermal annealing treatment at 100 °C was necessary. The thickness tolerance observed in PM7 D1 was observed in both North Carolina State University and Georgia Institute of Technology laboratories to provide evidence of reproducibility (Table 2, Fig. S25). Although the solar cell characteristics are slightly different, the values show a similar trend. Moreover, PM7 D1 (PCE = 10.6%) was found to have a better active layer thickness tolerance than PM7 (PCE = 8.3%), which suggests PM7 D1, when paired with

ITIC-4F, is the best candidate for large-scale processing of the three polymers reported here. Finally, 320 nm thick active layer devices were fabricated with each polymer to investigate if the thickness tolerance trend continues for each BHJ (Figure S26, Table 2). Predictably, the PCE for each device decreases due to a drop in FF. The PM7 D2:ITIC-4F blend's PCE continues to diminish (PCE < 4%) while PM7 D1's performance remains the highest of the three polymers at 8.8%. Indeed, PM7 D1's performance drops more significantly than PM7s, and therefore, the thickness tolerance difference becomes less significant around 300 nm. Regardless, the OSC performance differences between PM7 D1 and PM7 D2 are dramatic at all active layer thicknesses indicating significant morphological deviations as a result of the ester placement on the terthiophene moiety. The external quantum efficiency (EQE) spectra for all three polymer:ITIC-4F blends show similar results with minor differences between 300 to 810 nm, and all three show slightly higher integrated current when casted as a thicker film (Fig. S27 and Table S2).

Grazing-incidence wide-angle X-ray scattering (GIWAXS) was used to probe differences in molecular packing between PM7 D1 and D2 in attempts to understand the dissimilar active layer thickness tolerance in the OSC active layer blends.[89] The GIWAXS pristine and blend (thick and thin) 2D patterns are shown in Figure S28. The blend films were prepared using the same processing techniques as the solar cell active layers and the thin (100 nm) and thick (180 nm) films have similar thicknesses. In general, the PM7 D1 and D2 neat scattering patterns are very similar with preferential face-on π–π stacking orientation, as indicated by the pronounced (010) peak in the out-of-plane (OOP) direction and the corresponding high intensity (100) peak in the in-plane direction. Minor differences, as compared to the pristine polymer films, are observed in the blend GIWAXS patterns as the out-of-plane (010) reflection remains pronounced suggesting little disruption to the polymer organization by the ITIC-4F acceptor. Further, some insight into active

layer thickness tolerance differences between the two polymers can be gained when comparing the out-of-plane π–π stacking parameters, as shown in Table S3. Here, the π–π stacking of the PM7 D1 blend is unchanged and the coherence length changes from 27 Å to 32 Å, respectively, when comparing the thin and thick films. The PM7 D2 π–π stacking parameters change very little from a thin to thick film. However, the thickness and background normalized integrated intensity of the π-π stacking peak decreases in the D1 blends by a factor of 1.6 with an increase in thickness, whereas the intensities are similar in the D2 blend series (Fig. 4, Table S3). Although the π-π stacking peak intensity in the PM7 D2 blends is nearly unchanged, it showed a significant decrease in PCE with thickness, whereas the π-π stacking peak intensity of PM7 D1 decreased more considerably which ultimately translated to an unaffected PCE with thickness. This indicates that simple/traditional metrics of molecular packing that have worked in many other donor:acceptor material systems cannot be correlated to performance here.[90]

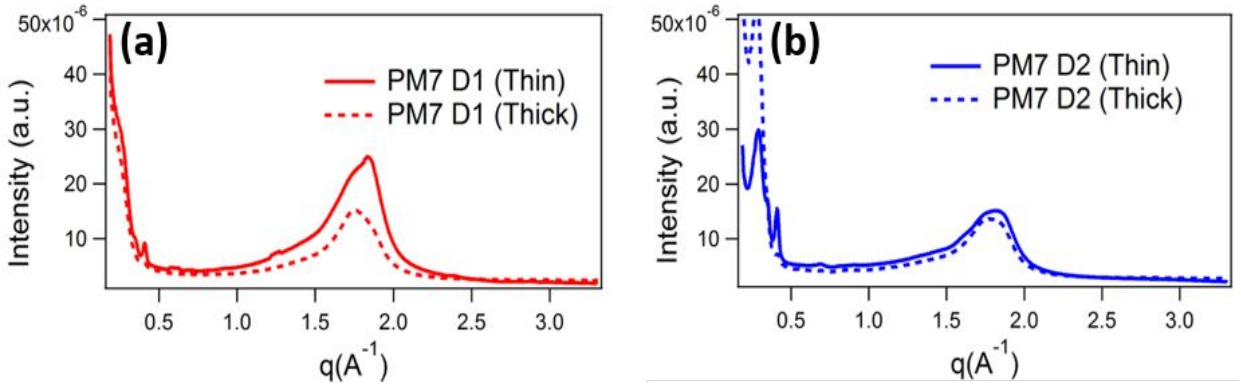

Figure 4. The out of plane GIWAXS line cuts for scatting volume normalized (a) PM7 D1 and (b) PM7 D2 blends.

To further probe the origin of the active layer thickness tolerance difference in the two PM7 derivatives, space-charge limited current (SCLC) measurements of hole and electron-only devices were carried out on the thick polymer:ITIC-4F blend films (Fig. S29). By fitting the J-V characteristics of single-carrier devices measured at room temperature, the hole mobility of all

BHJ blends show similar values ranging from 1.0×10^{-4} to 1.6×10^{-4} cm^2/Vs, while the BHJ film with PM7 D1 has roughly two times higher electron mobility than PM7 and PM7 D2 (Table 3). The higher electron mobility in the PM7 D1 BHJ blend results in a more balanced electron-hole mobility ratio, which accounts for the higher FF in PM7 D1 OPV devices.

Table 3. Summary of Mobility and Energetic Disorder of thick Polymer:ITIC-4F Blends

Polymer	Hole Mobility (cm^2/Vs)	Electron Mobility (cm^2/Vs)	σ_{hole} (meV)	$\sigma_{electron}$ (meV)
PM7	1.13×10^{-4}	2.67×10^{-5}	68	62
PM7 D1	1.64×10^{-4}	4.85×10^{-5}	65	62
PM7 D2	1.04×10^{-4}	2.34×10^{-5}	73	63

To further examine the transport behaviors of the BHJ films with different donor polymers, we performed temperature-dependent SCLC measurements to extract the energetic disorder parameter (σ) (Fig. S30). The resulting zero-field mobility at different temperatures (T) can be analyzed by the well accepted Gaussian disorder model (GDM) by a plot of extracted zero-field mobility (μ_0) against $1/T^2$ (Fig. 5).[91] According to the GDM, the temperature-dependent zero-field mobilities are related to T *via* Equation 1, where σ is the energetic disorder, μ_∞ is carrier mobility as temperature trends to infinity, and k represents the Boltzmann constant. In Eq. (1), μ_0, μ_∞, and σ can be associated with either electron (e) or hole (h) transport. Polymeric semiconductors have some level of disorder due to the different types of intra and intermolecular interactions that generate a

$$\mu_0 = \mu_\infty \exp[-(2\sigma/3kT)^2] \quad (1)$$

broadened electronic density-of-states (DOS).[92] Based on the polymeric backbone, side chains, and coupling with an electronic acceptor, different blend morphologies are generated due to the

conformational diversity of the molecular components.[93-94] These molecular interactions cause different levels of ordered and/or amorphous regions in the active layer film which ultimately affect the charge-transport properties of the BHJ. Typically, energetic disorder values range from 125 to 60 meV depending on the donor:acceptor materials, ratio, and processing thereof.[95-96] The extracted energetic disorders of the polymer:ITIC-4F blends are summarized in Table 3. The electron energetic disorder shows essentially no change between different BHJ blends, which is to be expected as ITIC-4F is the main electron transport pathway in the BHJ blends. In contrast, the hole energetic disorder for PM7 D2 is higher (73 meV) as compared to the other blends which reflects a distinct change in energy width of the hole hopping site manifold, which arises from interactions with its environment.[97-98] As such, we conclude the difference in performance of these OPVs originates from the different molecular packing properties that are occurring on the nm length-scale of the donor polymer. This is the first time, as far as we know, that the energetic disorder parameter has been correlated with the active layer thickness tolerance of polymeric donor materials.

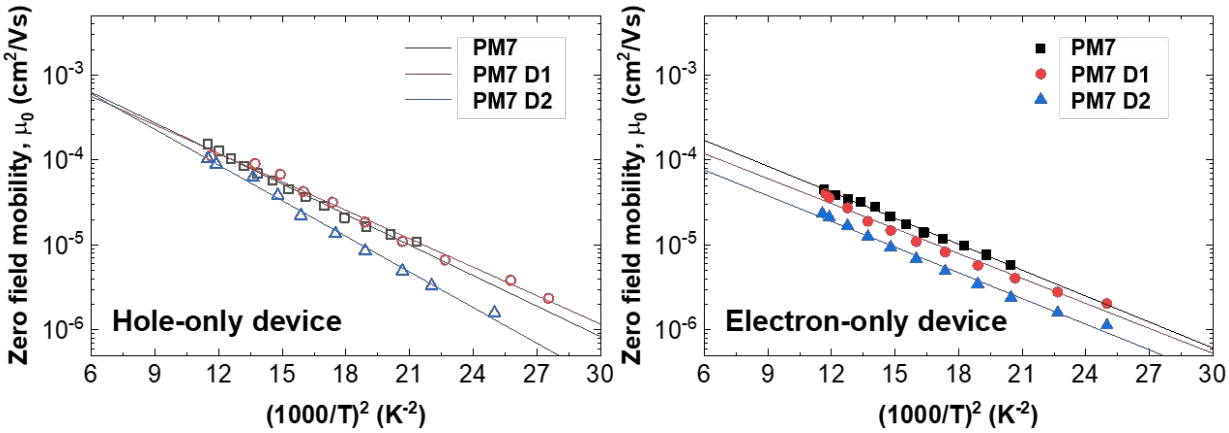

Figure 5. Zero-field mobilities vs $1/T^2$. Solid lines are best linear fits to the experimental data. The slopes of the plots yield the energetic disorders

3. Conclusion and Perspective

To conclude, two PM7 isomeric derivatives (PM7 D1 and PM7 D2), and PM7, were synthesized with similar molecular weights and dispersities to compare their OSC performance and active layer thickness tolerance when paired with the NFA ITIC-4F. As compared to PM7, the two derivatives have less-structured, blue-shifted absorption profiles indicative of a less-planar and aggregated configuration. Thin-film properties and OSC (100 nm) device performance yielded similar results for the family of polymers with PM7 (PCE = 12.1 ± 0.4) and PM7 D1 (PCE = 11.6 ± 0.5) demonstrating higher PCEs as compared to PM7 D2 (PCE = 9.9 ± 0.2). Conversely, large differences in device performance were observed when the active layer thickness was increased to 180 nm, where PM7 D1 was able to retain its PCE (PCE = 11.9 ± 0.2), but the PCE of PM7 D2 dramatically decreased (PCE= 5.3 ± 0.1). The GIWAX data indicated that the changes to the backbone repeat structure had little correlative relation of the average molecular packing and texture of the overall film to performance. The thickness tolerance difference between the two isomeric polymers was ultimately attributed to the higher energetic disorder in the hole transport for PM7 D2 (73 meV) as compared to PM7 D1 (65 meV). Importantly, we demonstrate how thin-film (100-150 nm) device performance could be misleading when suggesting a material could be used for large-scale device fabrication as the thickness tolerance will be essential for a materials ability to be industrially relevant. Furthermore, molecular interactions that disrupt charge transport and cause recombination traps in BHJs may be more detrimental to the FF and J_{SC} as the active layer thickness increases. These unfavorable interactions can go undetected with many of the traditional material characterizations such as light absorption, charge mobility, x-ray scattering patterns, and electrochemically derived energy levels, and therefore, using techniques to

investigate energetic disorder, and the underlying reasons therein, will become important in optimizing future OPVs.

Conflicts of Interest

There are no conflicts to declare.

Acknowledgments

We acknowledge Yusen Pei (North Carolina State University) for his thick active layer device fabrication. This work was supported by the Department of the Navy, Office of Naval Research grant numbers N00014-17-1-2243 (Reynolds), N00014-17-1-2242 (So), and N00014-17-1-2204 and N00014-20-1-2155 (Ade). X-ray data were acquired at beamline 7.3.3 at the Advanced Light Source, which is supported by the Director, Office of Science, Office of Basic Energy Sciences, of the U.S. Department of Energy under Contract No. DE-AC02-05CH11231.

References

1. Zhang, G.; Zhao, J.; Chow, P. C. Y.; Jiang, K.; Zhang, J.; Zhu, Z.; Zhang, J.; Huang, F.; Yan, H., Nonfullerene Acceptor Molecules for Bulk Heterojunction Organic Solar Cells. *Chem. Rev.* **2018,** *118* (7), 3447-3507.

2. Wadsworth, A.; Moser, M.; Marks, A.; Little, M. S.; Gasparini, N.; Brabec, C. J.; Baran, D.; McCulloch, I., Critical Review of the Molecular Design Progress in Non-Fullerene Electron Acceptors Towards Commercially Viable Organic Solar Cells. *Chem. Soc. Rev.* **2019,** *48* (6), 1596-1625.

3. Fu, H.; Wang, Z.; Sun, Y., Polymer Donors for High-Performance Non-Fullerene Organic Solar Cells. *Angew. Chem., Int. Ed.* **2019,** *58* (14), 4442-4453.

4. Gurney, R. S.; Lidzey, D. G.; Wang, T., A Review of Non-Fullerene Polymer Solar Cells: from Device Physics to Morphology Control. *Rep. Prog. Phys.* **2019,** *82* (3), 36601.

5. Lin, Y.; Adilbekova, B.; Firdaus, Y.; Yengel, E.; Faber, H.; Sajjad, M.; Zheng, X.; Yarali, E.; Seitkhan, A.; Bakr, O. M.; El-Labban, A.; Schwingenschloegl, U.; Tung, V.; McCulloch, I.; Laquai, F.; Anthopoulos, T. D., 17% Efficient Organic Solar Cells Based on Liquid Exfoliated WS2 as a Replacement for PEDOT:PSS. *Adv. Mater.* **2019,** *31* (46), 1902965.

6. Liu, L.; Kan, Y.; Gao, K.; Wang, J.; Zhao, M.; Chen, H.; Zhao, C.; Jiu, T.; Jen, A.-K. Y.; Li, Y., Graphdiyne Derivative as Multifunctional Solid Additive in Binary Organic Solar Cells with 17.3% Efficiency and High Reproductivity. *Adv. Mater.* **2020,** *32* (11), 1907604.

7. Zhan, L.; Li, S.; Lau, T.-K.; Cui, Y.; Lu, X.; Shi, M.; Li, C.-Z.; Li, H.; Hou, J.; Chen, H., Over 17% Efficiency Ternary Organic Solar Cells Enabled by Two Non-Fullerene Acceptors Working in an Alloy-Like Model. *Energy Environ. Sci.* **2020,** *13* (2), 635-645.

8. Ma, R.; Liu, T.; Luo, Z.; Guo, Q.; Xiao, Y.; Chen, Y.; Li, X.; Luo, S.; Lu, X.; Zhang, M.; Li, Y.; Yan, H., Improving Open-Circuit Voltage by a Chlorinated Polymer Donor Endows Binary Organic Solar Cells Efficiencies Over 17%. *Sci. China: Chem.* **2020,** *63* (3), 325-330.

9. Sun, C.; Qin, S.; Wang, R.; Chen, S.; Pan, F.; Qiu, B.; Shang, Z.; Meng, L.; Zhang, C.; Xiao, M.; Yang, C.; Li, Y., High Efficiency Polymer Solar Cells with Efficient Hole Transfer at Zero Highest Occupied Molecular Orbital Offset between Methylated Polymer Donor and Brominated Acceptor. *J. Am. Chem. Soc.* **2020,** *142* (3), 1465-1474.

10. Nielsen, C. B.; Holliday, S.; Chen, H.-Y.; Cryer, S. J.; McCulloch, I., Non-Fullerene Electron Acceptors for Use in Organic Solar Cells. *Acc. Chem. Res.* **2015,** *48* (11), 2803-2812.

11. Yan, C.; Barlow, S.; Wang, Z.; Yan, H.; Jen, A. K. Y.; Marder, S. R.; Zhan, X., Non-Fullerene Acceptors for Organic Solar Cells. *Nat. Rev. Mater.* **2018,** *3* (3), 18003.

12. Lin, Y.; Wang, J.; Zhang, Z.-G.; Bai, H.; Li, Y.; Zhu, D.; Zhan, X., An Electron Acceptor Challenging Fullerenes for Efficient Polymer Solar Cells. *Adv. Mater.* **2015,** *27* (7), 1170-1174.

13. Dai, S.; Zhao, F.; Zhang, Q.; Lau, T.-K.; Li, T.; Liu, K.; Ling, Q.; Wang, C.; Lu, X.; You, W.; Zhan, X., Fused Nonacyclic Electron Acceptors for Efficient Polymer Solar Cells. *J. Am. Chem. Soc.* **2017,** *139* (3), 1336-1343.

14. Lin, Y.; Zhao, F.; He, Q.; Huo, L.; Wu, Y.; Parker, T. C.; Ma, W.; Sun, Y.; Wang, C.; Zhu, D.; Heeger, A. J.; Marder, S. R.; Zhan, X., High-Performance Electron Acceptor with Thienyl Side Chains for Organic Photovoltaics. *J. Am. Chem. Soc.* **2016,** *138* (14), 4955-4961.

15. Lin, Y.; He, Q.; Zhao, F.; Huo, L.; Mai, J.; Lu, X.; Su, C.-J.; Li, T.; Wang, J.; Zhu, J.; Sun, Y.; Wang, C.; Zhan, X., A Facile Planar Fused-Ring Electron Acceptor for As-Cast Polymer Solar Cells with 8.71% Efficiency. *J. Am. Chem. Soc.* **2016,** *138* (9), 2973-2976.

16. Wang, J.; Zhang, J.; Xiao, Y.; Xiao, T.; Zhu, R.; Yan, C.; Fu, Y.; Lu, G.; Lu, X.; Marder, S. R.; Zhan, X., Effect of Isomerization on High-Performance Nonfullerene Electron Acceptors. *J. Am. Chem. Soc.* **2018,** *140* (29), 9140-9147.

17. Yao, Z.; Liao, X.; Gao, K.; Lin, F.; Xu, X.; Shi, X.; Zuo, L.; Liu, F.; Chen, Y.; Jen, A. K. Y., Dithienopicenocarbazole-Based Acceptors for Efficient Organic Solar Cells with Optoelectronic Response Over 1000 nm and an Extremely Low Energy Loss. *J. Am. Chem. Soc.* **2018,** *140* (6), 2054-2057.

18. Zhao, W.; Li, S.; Yao, H.; Zhang, S.; Zhang, Y.; Yang, B.; Hou, J., Molecular Optimization Enables over 13% Efficiency in Organic Solar Cells. *J. Am. Chem. Soc.* **2017,** *139* (21), 7148-7151.

19. Yuan, J.; Zhang, Y.; Zhou, L.; Zhang, G.; Yip, H.-L.; Lau, T.-K.; Lu, X.; Zhu, C.; Peng, H.; Johnson, P. A.; Leclerc, M.; Cao, Y.; Ulanski, J.; Li, Y.; Zou, Y., Single-Junction Organic

Solar Cell with over 15% Efficiency Using Fused-Ring Acceptor with Electron-Deficient Core. *Joule* **2019,** *3* (4), 1140-1151.

20. Ge, J.; Xie, L.; Peng, R.; Fanady, B.; Huang, J.; Song, W.; Yan, T.; Zhang, W.; Ge, Z.; Peng, R.; Yan, T.; Zhang, W.; Ge, Z., 13.34 % Efficiency Non-Fullerene All-Small-Molecule Organic Solar Cells Enabled by Modulating the Crystallinity of Donors via a Fluorination Strategy. *Angew. Chem. Int. Ed.* **2020,** *59* (7), 2808-2815.

21. Cui, Y.; Yao, H.; Zhang, J.; Zhang, T.; Wang, Y.; Hong, L.; Xian, K.; Xu, B.; Zhang, S.; Peng, J.; Wei, Z.; Gao, F.; Hou, J., Over 16% Efficiency Organic Photovoltaic Cells Enabled by a Chlorinated Acceptor with Increased Open-Circuit Voltages. *Nat. Commun.* **2019,** *10* (1), 1-8.

22. Cai, F.; Zhu, C.; Yuan, J.; Li, Z.; Meng, L.; Liu, W.; Peng, H.; Jiang, L.; Li, Y.; Zou, Y., Efficient Organic Solar Cells Based on a New "Y-Series" Non-Fullerene Acceptor with an Asymmetric Electron-Deficient-Core. *Chem. Commun.* **2020**, *56* (31), 4340-4343.

23. Zhou, Z.; Liu, W.; Zhou, G.; Zhang, M.; Qian, D.; Zhang, J.; Chen, S.; Xu, S.; Yang, C.; Gao, F.; Zhu, H.; Liu, F.; Zhu, X., Subtle Molecular Tailoring Induces Significant Morphology Optimization Enabling over 16% Efficiency Organic Solar Cells with Efficient Charge Generation. *Adv. Mater.* **2020,** *32* (4), 1906324.

24. Yuan, J.; Huang, T.; Cheng, P.; Zou, Y.; Zhang, H.; Yang, J. L.; Chang, S.-Y.; Zhang, Z.; Huang, W.; Wang, R.; Meng, D.; Gao, F.; Yang, Y., Enabling Low Voltage Losses and High Photocurrent in Fullerene-Free Organic Photovoltaics. *Nat. Commun.* **2019,** *10* (1), 570.

25. Qin, R.; Wang, D.; Zhou, G.; Yu, Z.-P.; Li, S.; Li, Y.; Liu, Z.-X.; Zhu, H.; Shi, M.; Lu, X.; Li, C.-Z.; Chen, H., Tuning Terminal Aromatics of Electron Acceptors to Achieve High-Efficiency Organic Solar Cells. *J. Mater. Chem. A* **2019,** *7* (48), 27632-27639.

26. Chen, S.; Liu, Y.; Zhang, L.; Chow, P. C. Y.; Wang, Z.; Zhang, G.; Ma, W.; Yan, H., A Wide-Bandgap Donor Polymer for Highly Efficient Non-fullerene Organic Solar Cells with a Small Voltage Loss. *J. Am. Chem. Soc.* **2017,** *139* (18), 6298-6301.

27. Zhao, F.; Dai, S.; Wu, Y.; Zhang, Q.; Wang, J.; Jiang, L.; Ling, Q.; Wei, Z.; Ma, W.; You, W.; Wang, C.; Zhan, X., Single-Junction Binary-Blend Nonfullerene Polymer Solar Cells with 12.1% Efficiency. *Adv. Mater.* **2017,** *29* (18), 1700144.

28. Li, S.; Ye, L.; Zhao, W.; Yan, H.; Yang, B.; Liu, D.; Li, W.; Ade, H.; Hou, J., A Wide Band Gap Polymer with a Deep Highest Occupied Molecular Orbital Level Enables 14.2% Efficiency in Polymer Solar Cells. *J. Am. Chem. Soc.* **2018,** *140* (23), 7159-7167.

29. Qian, D.; Ye, L.; Zhang, M.; Liang, Y.; Li, L.; Huang, Y.; Guo, X.; Zhang, S.; Tan, Z.; Hou, J., Design, Application, and Morphology Study of a New Photovoltaic Polymer with Strong Aggregation in Solution State. *Macromolecules* **2012,** *45* (24), 9611-9617.

30. Liu, D.; Yang, B.; Jang, B.; Xu, B.; Zhang, S.; He, C.; Woo, H. Y.; Hou, J., Molecular Design of a Wide-Band-Gap Conjugated Polymer for Efficient Fullerene-Free Polymer Solar Cells. *Energy Environ. Sci.* **2017,** *10* (2), 546-551.

31. Wang, Q.; Li, M.; Zhang, X.; Qin, Y.; Wang, J.; Zhang, J.; Hou, J.; Janssen, R. A. J.; Geng, Y., Carboxylate-Substituted Polythiophenes for Efficient Fullerene-Free Polymer Solar Cells: The Effect of Chlorination on Their Properties. *Macromolecules* **2019,** *52* (12), 4464-4474.

32. Li, S.; Zhao, W.; Zhang, J.; Liu, X.; Zheng, Z.; He, C.; Xu, B.; Wei, Z.; Hou, J., Influence of Covalent and Noncovalent Backbone Rigidification Strategies on the Aggregation Structures of a Wide-Band-Gap Polymer for Photovoltaic Cells. *Chem. Mater.* **2020,** *32* (5), 1993-2003.

33. Yao, H.; Cui, Y.; Qian, D.; Ponseca, C. S.; Honarfar, A.; Xu, Y.; Xin, J.; Chen, Z.; Hong, L.; Gao, B.; Yu, R.; Zu, Y.; Ma, W.; Chabera, P.; Pullerits, T.; Yartsev, A.; Gao, F.; Hou, J., 14.7%

Efficiency Organic Photovoltaic Cells Enabled by Active Materials with a Large Electrostatic Potential Difference. *J. Am. Chem. Soc.* **2019,** *141* (19), 7743-7750.

34. Zhu, J.; Liu, Q.; Li, D.; Xiao, Z.; Chen, Y.; Hua, Y.; Yang, S.; Ding, L., A Wide-Band Gap Copolymer Donor for Efficient Fullerene-Free Solar Cells. *ACS Omega* **2019,** *4* (12), 14800-14804.

35. Cui, Y.; Yao, H.; Hong, L.; Zhang, T.; Xu, Y.; Xian, K.; Gao, B.; Qin, J.; Zhang, J.; Wei, Z.; Hou, J., Achieving Over 15% Efficiency in Organic Photovoltaic Cells via Copolymer Design. *Adv. Mater.* **2019,** *31* (14), 1808356.

36. Zhao, W.; Qian, D.; Zhang, S.; Li, S.; Inganäs, O.; Gao, F.; Hou, J., Fullerene-Free Polymer Solar Cells with over 11% Efficiency and Excellent Thermal Stability. *Adv. Mater.* **2016,** *28* (23), 4734-4739.

37. Li, S.; Ye, L.; Zhao, W.; Zhang, S.; Mukherjee, S.; Ade, H.; Hou, J., Energy-Level Modulation of Small-Molecule Electron Acceptors to Achieve over 12% Efficiency in Polymer Solar Cells. *Adv. Mater.* **2016,** *28* (42), 9423-9429.

38. Zheng, Z.; Yao, H.; Ye, L.; Xu, Y.; Zhang, S.; Hou, J., PBDB-T and its Derivatives: A Family of Polymer Donors Enables over 17% Efficiency in Organic Photovoltaics. *Mater. Today* **2019**, *35*, 115-130.

39. Zhang, M.; Guo, X.; Ma, W.; Ade, H.; Hou, J., A Large-Bandgap Conjugated Polymer for Versatile Photovoltaic Applications with High Performance. *Adv. Mater.* **2015,** *27* (31), 4655-4660.

40. Hong, L.; Yao, H.; Yu, R.; Xu, Y.; Gao, B.; Ge, Z.; Hou, J., Investigating the Trade-Off between Device Performance and Energy Loss in Nonfullerene Organic Solar Cells. *ACS Appl. Mater. Interfaces* **2019,** *11* (32), 29124-29131.

41. Cui, Y.; Wang, Y.; Bergqvist, J.; Yao, H.; Xu, Y.; Gao, B.; Yang, C.; Zhang, S.; Inganäs, O.; Gao, F.; Hou, J., Wide-Gap Non-Fullerene Acceptor Enabling High-Performance Organic Photovoltaic Cells for Indoor Applications. *Nat. Energy* **2019,** *4* (9), 768-775.

42. Li, W.; Ye, L.; Li, S.; Yao, H.; Ade, H.; Hou, J., A High-Efficiency Organic Solar Cells Enabled by the Strong Intramolecular Electron Push-Pull Effect of the Nonfullerene Acceptor. *Adv. Mater.* **2018,** *30* (16), 1707170.

43. Ma, X.; Wang, J.; An, Q.; Gao, J.; Hu, Z.; Xu, C.; Zhang, X.; Liu, Z.; Zhang, F., Highly Efficient Quaternary Organic Photovoltaics by Optimizing Photogenerated Exciton Distribution and Active Layer Morphology. *Nano Energy* **2020,** *70*, 104496.

44. Song, J.; Li, C.; Zhu, L.; Guo, J.; Xu, J.; Zhang, X.; Weng, K.; Zhang, K.; Min, J.; Hao, X.; Zhang, Y.; Liu, F.; Sun, Y., Ternary Organic Solar Cells with Efficiency >16.5% Based on Two Compatible Nonfullerene Acceptors. *Adv. Mater.* **2019,** *31* (52), 1905645.

45. Zhang, Y.; Feng, H.; Meng, L.; Wang, Y.; Chang, M.; Li, S.; Guo, Z.; Li, C.; Zheng, N.; Xie, Z.; Wan, X.; Chen, Y., High Performance Thick-Film Nonfullerene Organic Solar Cells with Efficiency over 10% and Active Layer Thickness of 600 nm. *Adv. Energy Mater.* **2019,** *9* (45), 1902688.

46. Karki, A.; Vollbrecht, J.; Dixon, A. L.; Schopp, N.; Schrock, M.; Reddy, G. N. M.; Nguyen, T.-Q., Understanding the High Performance of over 15% Efficiency in Single-Junction Bulk Heterojunction Organic Solar Cells. *Adv. Mater.* **2019,** *31* (48), 1903868.

47. Su, D.; Pan, M.-A.; Liu, Z.; Lau, T.-K.; Li, X.; Shen, F.; Huo, S.; Lu, X.; Xu, A.; Yan, H.; Zhan, C., A Trialkylsilylthienyl Chain-Substituted Small-Molecule Acceptor with Higher LUMO Level and Reduced Band Gap for Over 16% Efficiency Fullerene-Free Ternary Solar Cells. *Chem. Mater.* **2019,** *31* (21), 8908-8917.

48. Yao, H.; Bai, F.; Hu, H.; Arunagiri, L.; Zhang, J.; Chen, Y.; Yu, H.; Chen, S.; Liu, T.; Lai, J. Y. L.; Zou, Y.; Ade, H.; Yan, H., Efficient All-Polymer Solar Cells based on a New Polymer Acceptor Achieving 10.3% Power Conversion Efficiency. *ACS Energy Lett.* **2019,** *4* (2), 417-422.

49. Zhang, Q.; Kelly, M. A.; Bauer, N.; You, W., The Curious Case of Fluorination of Conjugated Polymers for Solar Cells. *Acc. Chem. Res.* **2017,** *50* (9), 2401-2409.

50. Chen, T.-W.; Peng, K.-L.; Lin, Y.-W.; Su, Y.-J.; Ma, K.-J.; Hong, L.; Chang, C.-C.; Hou, J.; Hsu, C.-S., A Chlorinated Nonacyclic Carbazole-Based Acceptor Affords over 15% Efficiency in Organic Solar Cells. *J. Mater. Chem. A* **2020,** *8* (3), 1131-1137.

51. Ma, K.; An, C.; Zhang, T.; Lv, Q.; Zhang, S.; Zhou, P.; Zhang, J.; Hou, J., Study of Photovoltaic Performances for Asymmetrical and Symmetrical Chlorinated Thiophene-Bridge-Based Conjugated Polymers. *J. Mater. Chem. C* **2020,** *8* (7), 2301-2306.

52. Zhang, Y.; Yao, H.; Zhang, S.; Qin, Y.; Zhang, J.; Yang, L.; Li, W.; Wei, Z.; Gao, F.; Hou, J., Fluorination vs. Chlorination: a Case Study on High Performance Organic Photovoltaic Materials. *Sci. China: Chem.* **2018,** *61* (10), 1328-1337.

53. Zhang, H.; Yao, H.; Hou, J.; Zhu, J.; Zhang, J.; Li, W.; Yu, R.; Gao, B.; Zhang, S.; Hou, J., Over 14% Efficiency in Organic Solar Cells Enabled by Chlorinated Nonfullerene Small-Molecule Acceptors. *Adv. Mater.* **2018,** *30* (28), 1800613.

54. Zhang, S.; Qin, Y.; Zhu, J.; Hou, J., Over 14% Efficiency in Polymer Solar Cells Enabled by a Chlorinated Polymer Donor. *Adv. Mater.* **2018,** *30* (20), 1800868.

55. Chen, Y.; Jiang, X.; Chen, X.; Zhou, J.; Tang, A.; Geng, Y.; Guo, Q.; Zhou, E., Modulation of Three p-Type Polymers Containing a Fluorinated-Thiophene-Fused-Benzotriazole Unit To Pair with a Benzotriazole-Based Non-fullerene Acceptor for High VOC Organic Solar Cells. *Macromolecules* **2019,** *52* (22), 8625-8630.

56. Tang, A.; Song, W.; Xiao, B.; Guo, J.; Min, J.; Ge, Z.; Zhang, J.; Wei, Z.; Zhou, E., Benzotriazole-Based Acceptor and Donors, Coupled with Chlorination, Achieve a High VOC of 1.24 V and an Efficiency of 10.5% in Fullerene-Free Organic Solar Cells. *Chem. Mater.* **2019,** *31* (11), 3941-3947.

57. Qiu, B.; Chen, S.; Li, H.; Luo, Z.; Yao, J.; Sun, C.; Li, X.; Xue, L.; Zhang, Z.-G.; Yang, C.; Li, Y., A Simple Approach to Prepare Chlorinated Polymer Donors with Low-Lying HOMO Level for High Performance Polymer Solar Cells. *Chem. Mater.* **2019,** *31* (17), 6558-6567.

58. Wu, Y.; An, C.; Shi, L.; Yang, L.; Qin, Y.; Liang, N.; He, C.; Wang, Z.; Hou, J., The Crucial Role of Chlorinated Thiophene Orientation in Conjugated Polymers for Photovoltaic Devices. *Angew. Chem., Int. Ed.* **2018,** *57* (39), 12911-12915.

59. Chen, H.; Hu, Z.; Wang, H.; Liu, L.; Chao, P.; Qu, J.; Chen, W.; Liu, A.; He, F., A Chlorinated π-Conjugated Polymer Donor for Efficient Organic Solar Cells. *Joule* **2018,** *2* (8), 1623-1634.

60. Fan, Q.; Zhu, Q.; Xu, Z.; Su, W.; Chen, J.; Wu, J.; Guo, X.; Ma, W.; Zhang, M.; Li, Y., Chlorine Substituted 2D-Conjugated Polymer for High-Performance Polymer Solar Cells with 13.1% Efficiency via Toluene Processing. *Nano Energy* **2018,** *48*, 413-420.

61. Sun, C.; Pan, F.; Bin, H.; Xue, L.; Qiu, B.; Zhang, Z.-G.; Li, Y.; Sun, C.; Pan, F.; Bin, H.; Li, Y.; Zhang, J.; Wei, Z.; Li, Y., A Low Cost and High Performance Polymer Donor Material for Polymer Solar Cells. *Nat Commun* **2018,** *9* (1), 743.

62. Jia, X. e.; Liu, G.; Chen, S.; Li, Z.; Wang, Z.; Yin, Q.; Yip, H.-L.; Yang, C.; Duan, C.; Huang, F.; Cao, Y., Backbone Fluorination of Polythiophenes Improves Device Performance of Non-Fullerene Polymer Solar Cells. *ACS Appl. Energy Mater.* **2019,** *2* (10), 7572-7583.

63. Wadsworth, A.; Hamid, Z.; Bidwell, M.; Ashraf, R. S.; Khan, J. I.; Anjum, D. H.; Cendra, C.; Yan, J.; Rezasoltani, E.; Guilbert, A. A. Y.; Azzouzi, M.; Gasparini, N.; Bannock, J. H.; Baran, D.; Wu, H.; de Mello, J. C.; Brabec, C. J.; Salleo, A.; Nelson, J.; Laquai, F.; McCulloch, I., Progress in Poly (3-Hexylthiophene) Organic Solar Cells and the Influence of Its Molecular Weight on Device Performance. *Adv. Energy Mater.* **2018,** *8* (28), 1801001.

64. Baran, D.; Ashraf, R. S.; Hanifi, D. A.; Abdelsamie, M.; Gasparini, N.; Rohr, J. A.; Holliday, S.; Wadsworth, A.; Lockett, S.; Neophytou, M.; Emmott, C. J. M.; Nelson, J.; Brabec, C. J.; Amassian, A.; Salleo, A.; Kirchartz, T.; Durrant, J. R.; McCulloch, I., Reducing the Efficiency-Stability-Cost Gap of Organic Photovoltaics with Highly Efficient and Stable Small Molecule Acceptor Ternary Solar Cells. *Nat. Mater.* **2017,** *16* (3), 363-369.

65. Holliday, S.; Ashraf, R. S.; Wadsworth, A.; Baran, D.; Yousaf, S. A.; Nielsen, C. B.; Tan, C.-H.; Dimitrov, S. D.; Shang, Z.; Gasparini, N.; Alamoudi, M.; Laquai, F.; Brabec, C. J.; Salleo, A.; Durrant, J. R.; McCulloch, I., High-Efficiency and Air-Stable P3HT-Based Polymer Solar Cells with a New Non-Fullerene Acceptor. *Nat. Commun.* **2016,** *7*, 11585.

66. Qin, Y.; Uddin, M. A.; Chen, Y.; Jang, B.; Zhao, K.; Zheng, Z.; Yu, R.; Shin, T. J.; Woo, H. Y.; Hou, J., Highly Efficient Fullerene-Free Polymer Solar Cells Fabricated with Polythiophene Derivative. *Adv. Mater.* **2016,** *28* (42), 9416-9422.

67. Liang, Z.; Li, M.; Wang, Q.; Qin, Y.; Stuard, S. J.; Peng, Z.; Deng, Y.; Ade, H.; Ye, L.; Geng, Y., Optimization Requirements of Efficient Polythiophene:Nonfullerene Organic Solar Cells. *Joule* **2020,** *4* (6), 1278-1295.

68. Sun, H.; Liu, T.; Yu, J.; Lau, T.-K.; Zhang, G.; Zhang, Y.; Su, M.; Tang, Y.; Ma, R.; Liu, B.; Liang, J.; Feng, K.; Lu, X.; Guo, X.; Gao, F.; Yan, H., A Monothiophene Unit Incorporating

both Fluoro and Ester Substitution Enabling High-Performance Donor Polymers for Non-Fullerene Solar Cells with 16.4% Efficiency. *Energy Environ. Sci.* **2019,** *12* (11), 3328-3337.

69. Jin, Y.; Chen, Z.; Xiao, M.; Peng, J.; Fan, B.; Ying, L.; Zhang, G.; Jiang, X.-F.; Yin, Q.; Liang, Z.; Huang, F.; Cao, Y., Thick Film Polymer Solar Cells Based on Naphtho[1,2-c:5,6-c]bis[1,2,5]thiadiazole Conjugated Polymers with Efficiency over 11%. *Adv. Energy Mater.* **2017,** *7* (22), 1700944.

70. Zhang, G.; Zhang, K.; Yin, Q.; Jiang, X.-F.; Wang, Z.; Xin, J.; Ma, W.; Yan, H.; Huang, F.; Cao, Y., High-Performance Ternary Organic Solar Cell Enabled by a Thick Active Layer Containing a Liquid Crystalline Small Molecule Donor. *J. Am. Chem. Soc.* **2017,** *139* (6), 2387-2395.

71. Li, W.; Hendriks, K. H.; Roelofs, W. S. C.; Kim, Y.; Wienk, M. M.; Janssen, R. A. J., Efficient Small Bandgap Polymer Solar Cells with High Fill Factors for 300 nm Thick Films. *Adv. Mater.* **2013,** *25* (23), 3182-3186.

72. Sondergaard, R.; Hoesel, M.; Angmo, D.; Larsen-Olsen, T. T.; Krebs, F. C., Roll-to-Roll Fabrication of Polymer Solar Cells. *Mater. Today* **2012,** *15* (1-2), 36-49.

73. Liu, Y.; Zhao, J.; Li, Z.; Mu, C.; Ma, W.; Hu, H.; Jiang, K.; Lin, H.; Ade, H.; Yan, H., Aggregation and Morphology Control Enables Multiple Cases of High-Efficiency Polymer Solar Cells. *Nat. Commun.* **2014,** *5*, 5293.

74. Chen, Z.; Cai, P.; Chen, J.; Liu, X.; Zhang, L.; Lan, L.; Peng, J.; Ma, Y.; Cao, Y., Low Band-Gap Conjugated Polymers with Strong Interchain Aggregation and Very High Hole Mobility Towards Highly Efficient Thick-Film Polymer Solar Cells. *Adv. Mater.* **2014,** *26* (16), 2586-2591.

75. Li, D.; Xiao, Z.; Wang, S.; Geng, X.; Yang, S.; Fang, J.; Yang, H.; Ding, L., A Thieno[3,2-c]Isoquinolin-5(4H)-One Building Block for Efficient Thick-Film Solar Cells. *Adv. Energy Mater.* **2018,** *8* (20), 1800397.

76. Duan, C.; Peng, Z.; Colberts, F. J. M.; Pang, S.; Ye, L.; Awartani, O. M.; Hendriks, K. H.; Ade, H.; Wienk, M. M.; Janssen, R. A. J., Efficient Thick-Film Polymer Solar Cells with Enhanced Fill Factors via Increased Fullerene Loading. *ACS Appl. Mater. Interfaces* **2019,** *11* (11), 10794-10800.

77. Jiang, H.; Pan, F.; Zhang, L.; Zhou, X.; Wang, Z.; Nian, Y.; Liu, C.; Tang, W.; Ma, Q.; Ni, Z.; Chen, M.; Ma, W.; Cao, Y.; Chen, J., Impact of the Siloxane-Terminated Side Chain on Photovoltaic Performances of the Dithienylbenzodithiophene-Difluorobenzotriazole-Based Wide Band Gap Polymer Donor in Non-Fullerene Polymer Solar Cells. *ACS Appl. Mater. Interfaces* **2019,** *11* (32), 29094-29104.

78. Feng, S.; Zhang, C. e.; Bi, Z.; Liu, Y.; Jiang, P.; Ming, S.; Xu, X.; Ma, W.; Bo, Z., Controlling Molecular Packing and Orientation via Constructing a Ladder-Type Electron Acceptor with Asymmetric Substituents for Thick-Film Nonfullerene Solar Cells. *ACS Appl. Mater. Interfaces* **2019,** *11* (3), 3098-3106.

79. Luo, Z.; Sun, C.; Chen, S.; Zhang, Z.-G.; Wu, K.; Qiu, B.; Yang, C.; Li, Y.; Yang, C., Side-Chain Impact on Molecular Orientation of Organic Semiconductor Acceptors: High Performance Nonfullerene Polymer Solar Cells with Thick Active Layer over 400 nm. *Adv. Energy Mater.* **2018,** *8* (23), 1800856.

80. Wang, J.-L.; Liu, K.-K.; Hong, L.; Ge, G.-Y.; Zhang, C.; Hou, J., Selenopheno[3,2-b]thiophene-Based Narrow-Bandgap Nonfullerene Acceptor Enabling 13.3% Efficiency for

Organic Solar Cells with Thickness-Insensitive Feature. *ACS Energy Lett.* **2018,** *3* (12), 2967-2976.

81. Gao, J.; Gao, W.; Ma, X.; Hu, Z.; Xu, C.; Wang, X.; An, Q.; Yang, C.; Zhang, X.; Zhang, F., Over 14.5% Efficiency and 71.6% Fill Factor of Ternary Organic Solar Cells with 300 nm Thick Active Layers. *Energy Environ. Sci.* **2020,** *13* (3), 958-967.

82. Zhang, L.; Yi, N.; Zhou, W.; Yu, Z.; Liu, F.; Chen, Y., Miscibility Tuning for Optimizing Phase Separation and Vertical Distribution toward Highly Efficient Organic Solar Cells. *Adv. Sci.* **2019,** *6* (15), 1900565.

83. Ma, L.; Xu, Y.; Zu, Y.; Liao, Q.; Xu, B.; An, C.; Zhang, S.; Hou, J., A Ternary Organic Solar Cell with 300 nm Thick Active Layer shows Over 14% Efficiency. *Sci. China: Chem.* **2020,** *63* (1), 21-27.

84. Jones, A. L.; Gish, M. K.; Zeman, C. J.; Papanikolas, J. M.; Schanze, K. S., Photoinduced Electron Transfer in Naphthalene Diimide End-Capped Thiophene Oligomers. *J. Phys. Chem. A* **2017,** *121* (50), 9579-9588.

85. Jones, A. L.; Zheng, Z.; Riley, P.; Pelse, I.; Zhang, J.; Abdelsamie, M.; Toney, M. F.; Marder, S. R.; So, F.; Brédas, J.-L.; Reynolds, J. R., Acceptor Gradient Polymer Donors for Non-Fullerene Organic Solar Cells. *Chem. Mater.* **2019,** *31* (23), 9729-9741.

86. Willems, R. E. M.; Weijtens, C. H. L.; de Vries, X.; Coehoorn, R.; Janssen, R. A. J., Relating Frontier Orbital Energies from Voltammetry and Photoelectron Spectroscopy to the Open-Circuit Voltage of Organic Solar Cells. *Adv. Energy Mater.* **2019,** *9* (10), 1803677.

87. Zhang, Z.; Wang, H.; Yu, J.; Sun, R.; Xu, J.; Yang, L.; Geng, R.; Cao, J.; Du, F.; Min, J.; Liu, F.; Tang, W., Modification on the Indacenodithieno[3,2-b]thiophene Core to Achieve Higher

Current and Reduced Energy Loss for Nonfullerene Solar Cells. *Chem. Mater.* **2020,** *32* (3), 1297-1307.

88. Lin, Y.-C.; Chen, C.-H.; Li, R.-H.; Tsao, C.-S.; Saeki, A.; Wang, H.-C.; Chang, B.; Huang, L.-Y.; Yang, Y.; Wei, K.-H., Atom-Varied Side Chains in Conjugated Polymers Affect Efficiencies of Photovoltaic Devices Incorporating Small Molecules. *ACS Appl. Polym. Mater.* **2020,** *2* (2), 636-646.

89. Hexemer, A.; Bras, W.; Glossinger, J.; Schaible, E.; Gann, E.; Kirian, R.; MacDowell, A.; Church, M.; Rude, B.; Padmore, H., A SAXS/WAXS/GISAXS Beamline with Multilayer Monochromator. *Journal of Physics.: Conf. Series* **2010,** *247*, 012007.

90. Hu, H.; Jiang, K.; Chow, P. C. Y.; Ye, L.; Zhang, G.; Li, Z.; Carpenter, J. H.; Ade, H.; Yan, H., Influence of Donor Polymer on the Molecular Ordering of Small Molecular Acceptors in Nonfullerene Polymer Solar Cells. *Adv. Energy Mater.* **2018,** *8* (5), 1701674.

91. Baranovskii, S. D., Theoretical Description of Charge Transport in Disordered Organic Semiconductors. *Phys. Status Solidi B* **2014,** *251* (3), 487-525.

92. Karki, A.; Wetzelaer, G.-J. A. H.; Reddy, G. N. M.; Nadazdy, V.; Seifrid, M.; Schauer, F.; Bazan, G. C.; Chmelka, B. F.; Blom, P. W. M.; Nguyen, T.-Q., Unifying Energetic Disorder from Charge Transport and Band Bending in Organic Eemiconductors. *Adv. Funct. Mater.* **2019,** *29* (20), 1901109.

93. Athanasopoulos, S.; Bassler, H.; Kohler, A., Disorder vs. Delocalization: Which Is More Advantageous for High-Efficiency Organic Solar Cells? *J. Phys. Chem. Lett.* **2019,** *10* (22), 7107-7112.

94. Kupgan, G.; Chen, X.-K.; Brédas, J.-L., Low Energetic Disorder in Small-Molecule Non-Fullerene Electron Acceptors. *ACS Mater. Lett.* **2019,** *1* (3), 350-353.

95. Yi, X.; Gautam, B.; Constantinou, I.; Cheng, Y.; Peng, Z.; Klump, E.; Ba, X.; Ho, C. H. Y.; Dong, C.; Marder, S. R.; Reynolds, J. R.; Tsang, S.-W.; Ade, H.; So, F., Impact of Nonfullerene Molecular Architecture on Charge Generation, Transport, and Morphology in PTB7-Th-Based Organic Solar Cells. *Adv. Funct. Mater.* **2018,** *28* (32), 1802702.

96. Perdigon-Toro, L.; Zhang, H.; Markina, A.; Yuan, J.; Hosseini, S. M.; Wolff, C. M.; Zuo, G.; Stolterfoht, M.; Zou, Y.; Gao, F.; Andrienko, D.; Shoaee, S.; Neher, D., Barrierless Free Charge Generation in the High-Performance PM6:Y6 Bulk Heterojunction Non-Fullerene Solar Cell. *Adv. Mater.* **2020,** *32* (9), 1906763.

97. Sit, W.-Y.; Cheung, S. H.; Chan, C. Y. H.; Tsung, K. K.; Tsang, S. W.; So, S. K., Probing Bulk Transport, Interfacial Disorders, and Molecular Orientations of Amorphous Semiconductors in a Thin-Film Transistor Configuration. *Adv. Electron. Mater.* **2016,** *2* (3), 1500273.

98. Xu, B.; Yi, X.; Huang, T.-Y.; Zheng, Z.; Zhang, J.; Salehi, A.; Coropceanu, V.; Ho, C. H. Y.; Marder, S. R.; Toney, M. F.; Brédas, J.-L.; So, F.; Reynolds, J. R., Donor Conjugated Polymers with Polar Side Chain Groups: The Role of Dielectric Constant and Energetic Disorder on Photovoltaic Performance. *Adv. Funct. Mater.* **2018,** *28* (46), 1803418.

TOC Graphic

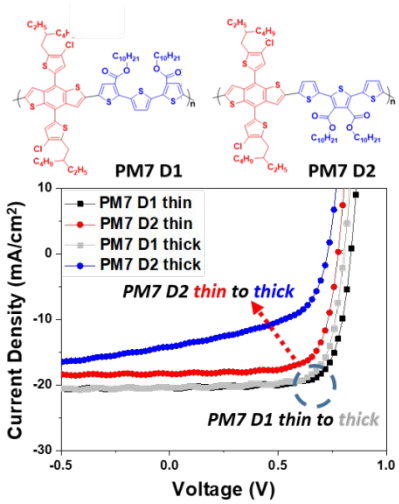
PM7 D1
PM7 D2
PM7 D1 thin
PM7 D2 thin
PM7 D1 thick
PM7 D2 thick
PM7 D2 thin to thick
PM7 D1 thin to thick
Current Density (mA/cm²)
Voltage (V)
10
0
-10
-20
-30
-0.5
0.0
0.5
1.0